Effect of Transverse Base Width Restraint on the Cracking Behavior of Massive Concrete

Dr. Adnan Falih. Ali
Professor
Baghdad University
Email:adnan.f@yahoo.com

Dr. Omar Al-Farouq Al-Damluji
Professor
Baghdad University
Email:omaraldamluji@gmail.com

Dr. Ala'a Hussein. A. Al-Zuhairi
Lecturer
Baghdad University
Email: alaalwn@yahoo.com

Abstract

The effect of considering the third dimension in mass concrete members on its cracking behavior is investigated in this study. The investigation includes thermal and structural analyses of mass concrete structures. From thermal analysis, the actual temperature distribution throughout the mass concrete body was obtained due to the generation of heat as a result of cement hydration in addition to the ambient circumstances. This was performed via solving the differential equations of heat conduction and convection using the finite element method.

The finite element method was also implemented in the structural analysis adopting the concept of initial strain problem. Drying shrinkage volume changes were calculated using the procedure suggested by ACI Committee 209 and inverted to equivalent temperature differences to be added algebraically to the temperature differences obtained from thermal analysis.

Willam-Warnke model with five strength parameters is used in modeling of concrete material in which cracking and crushing behavior of concrete can be included. The ANSYS program was employed in a modified manner to perform the above analyses.

A thick concrete slab of 1.5m in thickness and 10m in length was analyzed for different widths 2, 4, 8, and 10m to produce different aspect ratios (B/L) of 0.2, 0.4, 0.8, and 1.0 respectively. The results of the analyses show an increase in cracking tendency of mass concrete member as the aspect ratio of the same member is increased due to the effect of transverse base restraint. Accordingly, such effect cannot be ignored in the analysis of base restrained mass concrete structures subjected to temperature and drying shrinkage volume changes.

Keywords: Mass concrete, temperature difference, drying volume change, base restraint, concrete cracking.

تأثير تقييد عرض القاعدة العرضي على سلوك تشقق الخرسانة الكتلية

د.عدنان فالح علي
استاذ

د.عمرالفاروق الدملوجي
استاذ

د.علاء حسين علوان الزهيري
مدرس

الخلاصة

في هذا البحث، تم إجراء تحري عن تأثير أخذ البعد الثالث في أعضاء الخرسانة الكتلية بنظر الاعتبار على تـشققها. وتتضمن الدراسة إجراء التحليل الحراري والإنشائي لمنشآت الخرسانة الكتلية. ويتم الحصول على التوزيع الحقيقي لـ درجات الحرارة خلال جسم الخرسانة الكتلية من خلال التحليل الحراري للمسألة نتيجة للحرارة المتولدة جراء إماهة السمنت بالإضـافة إلى الظروف الجوية المحيطة. وهذا يجرى من خلال حل المعادلتين التفاضليتين للتوصيل والحمل الحراري باستخدام طريقـة العناصر المحددة.

كما إن طريقة العناصر المحددة أستخدمت أيضا في التحليل الأنشائي وذلك بتبني فكرة مسألة الأنفعال الابتدائي. كذلك يتم احتساب التقلصات الحجمية المرافقة لجفاف الخرسانة بالاعتماد على الطريقة المقترحة من قبل معهد الخرسانة الأمريكـي

لجنة 209 والتي يتم تحويلها إلى ما يكافئها من تغير في درجات الحرارة لتضاف جبريا إلى التغيرات بدرجات الحرارة التي تم الحصول عليها من التحليل الحراري.

لقد تم تبني نموذج ويلام-ورانك ذات خمسة معاملات مقاومة لتمثيل مادة الخرسانة إذ يتضمن هذا النموذج تصرف الخرسـانة في حالتي التشقق والتهشم. هذا وتم استخدام برنامج ANSYS وبطريقة معدلة لإنجاز التحليلين المشار اليهما أعلاه.

تم تحليل بلاطة خرسانية بسمك 1.5م وطـول 10م وبـأعراض مختلفـة 2، 4، 8 و10م لتحقيـق نـسب جانبيـة عرض/طول مختلفة 0.2، 0.4، 0.8و 1.0 على الترتيب. أظهرت نتائج التحليل زيادة في قابلية تشقق أعضاء الخرسانة الكتلية بزيادة النسب الجانبية بسبب تأثير تقييد القاعدة العرضي. وعليه، فأن مثل هذا التأثير لا يمكن إهماله فـي منـشآت الخرسـانة الكتلية التي تتعرض لتغيرات في درجات الحرارة و تقاص الجفاف.

الكلمات الرئيسيه :

الخرسانة الكتلية، اختلاف درجة الحرارة، التغير الحجمي بالجفاف، تقييد القاعدة، تشقق الخرسانة

Introduction

Mass concrete is an expression usually used for any concrete structure with dimensions large enough to cause structural problems during and after the construction period. These problems are mainly the occurrence of cracking due to temperature variations and shrinkage volume changes. Like any solid material, concrete is affected by increase and decrease of temperature. The effect appears as a thermal strain that occurs within the concrete structure when it is prevented or restricted from motion, i.e., restrained. The second category of volume change is the drying shrinkage, which is related to the drying and shrinking of the cement gel.

ACI 207 Committee (ACI Committee 1995) suggested the following equations to be Used to calculate the degree of restraint for rigid continuous base restraint.

$$K_R = [(L/H-2)/(L/H+1)]^{h/H} \quad for\, L/H \geq 2.5$$
$$K_R = [(L/H-1)/(L/H+10)]^{h/H} \quad for\, L/H < 2.5 \qquad (1)$$

Where

K_R = degree of restraint
L/H = length to height ratio, and
h = the height at which the degree of restraint is calculated.

As can be noticed, ACI 207 Committee neglects the effect of the restraint in the transverse direction and hence, eq. (1) can be applied to the concrete walls only. Therefore, it is the objective of the present study to investigate the effect of transverse base restraint, i.e., effects of 3rd dimension on the behavior of massive concrete and therefore cracking tendency and cracking prevention in such structures.

Thermal Analysis

Based on Fourier's Law for heat transfer, the heat conduction equation can be expressed as follows (Holman, 1981):

$$k_x \frac{\partial^2 T}{\partial x^2} + k_y \frac{\partial^2 T}{\partial y^2} + k_z \frac{\partial^2 T}{\partial z^2} + \overline{q} = \rho c_p \frac{\partial T}{\partial t} \qquad (2)$$

where,

k_x, k_y and k_z = heat conductivity of the material in x, y and z-direction respectively,

T = the difference between absolute and reference temperatures,

$\overline{q}$ = heat generation per unit volume,

c_p = specific heat, and

ρ = density.

On the other hand, heat may transfer by convection according to the following Newton formula (Holman, 1981):

$$q = \int_A h_{cv}(T - T_\infty) dA \qquad (3)$$

where,

h_{cv} = convection heat transfer coefficient (film coefficient).

T_∞ = bulk fluid temperature.

T = temperature.

Both of the above equations may be descritized using Raylieh-Ritz variation process to derive an expression employing the finite difference method to overcome the time-rate nature of the problem, that is,

$$\left[K_e^*\right]\left\{\Delta\delta_{(t)}\right\}=\left\{F^*\right\} \quad (4)$$

where,

$$\left[K_e^*\right]=\left[K_e\right]+\frac{[C]}{\Delta t}$$

$$\left\{F^*\right\}=\left\{\Delta F_{(t)}\right\}+\frac{[C]}{\Delta t}\left\{\Delta\delta_{(t-\Delta t)}\right\}$$

Eq. (4) is used in the finite element method to predict the temperature distribution within the mass concrete body invoking the described initial and boundary temperatures as follows:

1. Initial temperature = concrete placement temperature = 20 ^{o}C.
2. Bulk ambient temperature T_∞ which is specified for Baghdad climate according to Kammouna, 2001, from:

$$T_\infty = 29.815 - 15.291*\cos(0.893t \quad (5)$$

Where, t is time in days.

Shrinkage Strain Calculation

Following the procedure recommended by (ACI Committee 209, 1992) and taking the ambient circumstances and concrete mixing and placing conditions, the drying shrinkage strains may be calculated as a function of time after curing period for concrete which is assumed to be seven days.

Quoting the concept of evaporable moisture content that was adopted by Carlson, 1937, the distribution of drying shrinkage strains may be assessed within the body of mass concrete member. Table (1) shows such distribution in which the values of drying shrinkage strains seem very low. Such observation may be related to the non-convenience of eq. (6) that was suggested by ACI 209 Committee (ACI Committee, 1992) and used to estimate shrinkage strain-time relation.

$$\left(\varepsilon_{sh}\right)_t=\frac{t}{35+t}\ \left(\varepsilon_{sh}\right)_u \quad (6)$$

where,

$(\varepsilon_{sh})_t$ = shrinkage strain at any time t (in days), and

$(\varepsilon_{sh})_u$ = ultimate shrinkage strain = $780*10^{-6}$.

As can be seen from eq. (6) 50% only of the ultimate shrinkage strain occurs at 35 days after curing. However, one can conclude from the trend of the drying shrinkage strains as they are decreased with the increase in the width of the slab as the major cause of cracking in large mass concrete members is the temperature variation rather than shrinkage volume changes.

Adopted Costitutive Relationship For Concrete

The concrete was modeled using Willam and Wranke model (Willam and Wranke, 1974) which predicts failure of brittle materials in which the cracking and crushing modes should be accounted for. The criterion for failure of concrete due to a multiaxial stress state can be expressed in the form:

$$\frac{F}{f_c'}-S\geq 0 \quad (7)$$

where,

F = a function of the principal stress state (σ_{xp}, σ_{yp}, σ_{zp}),

S = failure surface expressed in terms of principal stresses and five input strength parameters as follows:

f_t' = ultimate uniaxial tensile strength in MPa

f_c' = ultimate uniaxial compressive crushing strength in MPa,

f_{cb} = ultimate biaxial compressive strength in Mpa,

σ_h = ambient hydrostatic stress state in MPa,

f_1 = ambient hydrostatic stress state of biaxial superimposed on hydrostatic stress state in Mpa, and

f_2 = ambient hydrostatic stress state of uniaxial superimposed on hydrostatic stress state in Mpa.

For simplicity, Willam and Warnke, 1974, suggested the following equations to calculate three of strength parameters in terms of f_c' in case of $\left|\sigma_h\right|\leq\sqrt{3}f_c'$. Thus, the failure surface S can be specified with a minimum two constants, f_t' and f_c'.

$$f_{cb} = 1.2\, f_c'$$
$$f_1 = 1.45\, f_c' \qquad (8)$$
$$f_2 = 1.725\, f_c'$$

Failure of concrete is categorized into four domains. In each domain, independent functions were specified to describe the function F and the failure surface S. The failure surface S can be seen in Fig. (1).

Compression-Compression-Compression Domain($0 \le \sigma_1 \le \sigma_2 \le \sigma_3$)

In this case, F takes the form:

$$F = F_1 = \frac{1}{\sqrt{15}}\left[(\sigma_1 - \sigma_2)^2 + (\sigma_2 - \sigma_3)^2 + (\sigma_3 - \sigma_1)^2\right]^{\frac{1}{2}} \qquad (9)$$

and the failure surface S is defined as:

$$S = S_1 = \frac{2r_2\left(r_2^2 - r_1^2\right)\cos\eta + r_2(2r_1 - r_2)\left[4\left(r_2^2 - r_1^2\right)\cos^2\eta + 5r_1^2 - 4r_1 r_2\right]^{\frac{1}{2}}}{4\left(r_2^2 - r_1^2\right)\cos^2\eta + (r_2 - 2r_1)^2} \qquad (10)$$

where,

$$\cos\eta = \frac{2\sigma_1 - \sigma_2 - \sigma_3}{\sqrt{2}\left[(\sigma_1 - \sigma_2)^2 + (\sigma_2 - \sigma_3)^2 + (\sigma_3 - \sigma_1)^2\right]^{\frac{1}{2}}}$$

in which η = angle of similarity, and

$$r_1 = a_0 + a_1\xi + a_2\xi^2$$
$$r_2 = b_0 + b_1\xi + b_2\xi^2$$
$$\xi = \frac{\sigma_h}{f_c'}$$

The undetermined coefficients a_0, a_1, a_2, b_0, b_1, and b_2 are discussed below.

When $\eta = 0^o$, S_1 in eq. (10) is equal to r_1 while if $\eta = 60^o$, S_1 is equal to r_2. Therefore, the function r_1 represents the failure surface of all stress states with $\eta = 0^o$.

The function r_1 is determined by adjusting a_0, a_1, and a_2 such that f_t', f_{cb} and f_1 all lie on the failure surface. Mathematically:

$$\begin{Bmatrix} \frac{F_1}{f_c'}\left(\sigma_1 = f_t', \sigma_2 = \sigma_3 = 0\right) \\ \frac{F_1}{f_c'}\left(\sigma_1 = 0, \sigma_2 = \sigma_3 = -f_{cb}\right) \\ \frac{F_1}{f_c'}\left(\sigma_1 = -\sigma_h^a, \sigma_2 = \sigma_3 = -\sigma_h^a - f_1\right) \end{Bmatrix} = \begin{bmatrix} 1 & \xi_t & \xi_t^2 \\ 1 & \xi_{cb} & \xi_{cb}^2 \\ 1 & \xi_1 & \xi_1^2 \end{bmatrix} \begin{Bmatrix} a_0 \\ a_1 \\ a_2 \end{Bmatrix} \qquad (11)$$

In which:

$$\xi_t = \frac{f_t'}{3f_c'}\ ,\ \xi_{cb} = \frac{f_{cb}}{3f_c'}\ ,\ and\ \xi_1 = -\frac{\sigma_h^a}{f_c'} - \frac{2f_1}{3f_c'}\ .$$

The proper values for the coefficient a_0, a_1, and a_2 can be determined through the solution of the simultaneous equations given in eq. (11).

The function r_2 is calculated by adjusting b_0, b_1, and b_2 to satisfy the conditions:

$$\begin{Bmatrix} \frac{F_1}{f_c'}(\sigma_1=\sigma_2=0,\sigma_3=-f_c') \\ \frac{F_1}{f_c'}(\sigma_1=\sigma_2=-\sigma_h^a,\sigma_3=-\sigma_h^a-f_2) \\ 0 \end{Bmatrix} = \begin{bmatrix} 1 & -\frac{1}{3} & \frac{1}{9} \\ 1 & \xi_2 & \xi_2^2 \\ 1 & \xi_0 & \xi_0^2 \end{bmatrix} \begin{Bmatrix} b_0 \\ b_1 \\ b_2 \end{Bmatrix} \quad (12)$$

Where,

ξ_2 is defined by: $\xi_2 = -\frac{\sigma_h^a}{f_c'} - \frac{f_2}{3f_c'}$.

and ξ_0 is the positive root of the equation:

$$r_2(\xi_0) = a_0 + a_1\xi_0 + a_2\xi_0^2 \quad (13)$$

in which a_0, a_1, and a_2 are evaluated by eq. (11).

Since the failure surface must remain convex, the ratio r_1/r_2 is restricted to the range ($0.5<r_1/r_2<1.25$), although the upper bound is not considered to restriction since ($r_1/r_2 < 1.0$) for most materials. Also, the coefficients a_0, a_1, a_2, b_0, b_1, and b_2 must satisfy the conditions:

$a_0 > 0$, $a_1 \le 0$, $a_2 \le 0$

$b_0 > 0$, $b_1 \le 0$, $b_2 \le 0$

Therefore, the failure surface is closed and predicts failure under high hydrostatic pressure ($\xi < \xi_2$). This closure of the failure surface has not been verified experimentally and it has been suggested that Von Mises type cylinder is a more valid failure surface for large compressive σ_h-values. Consequently, it is recommended that values of f_1 and f_2 are selected at a hydrostatic stress level in the vicinity of or above the expected maximum hydrostatic stress encountered in the structure.

Eq. (9) describes the condition that the failure surface has an apex at $\xi = \xi_0$. A profile of r_1 and r_2 as a function of ξ is shown in Fig. (2).The lower curve represents all stress state such that $\eta = 0^o$ while the upper curve represents stress state such that $\eta = 60^o$. If the failure criterion is satisfied, the material is assumed to crush.

Tension-Compression-Compression Domain ($\sigma_1 \ge 0 \ge \sigma_2 \ge \sigma_3$)

In this regime, F takes the form:

$$F = F_2 = \frac{1}{\sqrt{15}}\left[(\sigma_2-\sigma_3)^2 + \sigma_2^2 + \sigma_3^2\right]^{\frac{1}{2}} \quad (14)$$

and S is defined as:

$$S = S_2 = \left(1 - \frac{\sigma_1}{f_t'}\right)\frac{2p_2(p_2^2-p_1^2)\cos\eta + p_2(2p_1-p_2)\left[4(p_2^2-p_1^2)\cos^2\eta + 5p_1^2 - 4p_1p_2\right]^{\frac{1}{2}}}{4(p_2^2-p_1^2)\cos^2\eta + (p_2-2p_1)^2} \quad (15)$$

where $\cos\eta$ is already defined above, and

$$p_1 = a_0 + a_1\chi + a_2\chi^2$$

$$p_2 = b_0 + b_1\chi + b_2\chi^2$$

$$\chi = \frac{1}{3}(\sigma_2+\sigma_3)$$

The coefficients a_0, a_1, a_2, b_0, b_1, and b_2 are defined by eq. (11) and eq. (12).

If the failure criterion is satisfied, cracking occurs in the plane perpendicular to the principal stress σ_1.

Tension- Tension -Compression Domain ($\sigma_1 \ge \sigma_2 \ge 0 \ge \sigma_3$)

Here the function F takes the form:

$$F = F_3 = \sigma_i \;\; ; i = 1,2 \quad (16)$$

and the failure surface S is defined as:

$$S = S_3 = \frac{f_t'}{f_c'}\left(1 + \frac{\sigma_3}{S_2(\sigma_i 0,\sigma_3)}\right); i = 1,2 \quad (17)$$

If the failure criterion for both i = 1, 2 is satisfied, cracking occur in the planes perpendicular to principal stresses σ_1, σ_2. If the failure criterion is satisfied only for i = 1, cracking occurs only in the plane perpendicular to principal stress σ_1.

Tension- Tension - Tension Domain ($\sigma_1 \geq \sigma_2 \geq 0 \geq \sigma_3$)

In this regime, F takes the form:

$$F = F_4 = \sigma_i \quad ; i = 1,2,3 \tag{18}$$

and S is defined as:

$$S = S_4 = \frac{f_t'}{f_c'} \tag{19}$$

If the failure criterion is satisfied in directions1, 2, and 3, cracking occurs in the planes perpendicular to principal stresses σ_1, σ_2, and σ_3, otherwise, cracking occurs in plane or plane

Perpendicular to the directions of principal stresses where the failure criterion is satisfied.

Implementation of the Finite Element Method

According to Fung, 1965, the effect of temperature changes on an elastic body subjected to external forces may be determined using one of the followings:

1. Solution of the discretized form of the coupled thermo-elastic equation in which the effect of both temperature and displacement on each other may be determined, i.e. the displacement due to unit temperature change and vice versa. However, this procedure is not usually used especially in problems where the temperature changes are not high enough like in mass concrete problem.
2. When the simplifying assumptions mentioned in (1) above are introduced, the theory is referred to as an uncoupled, quasi-static theory; it degenerates into heat conduction and thermoelasticity as two separate problems. Experience shows that the change of temperature of an elastic body due to adiabatic straining is, in general, very small. If this interaction between strain and temperature is ignored, then the only effects of elasticity on the temperature distribution are effects of change in dimensions of the body under investigation. The change in dimension of a body is of the order of product of the linear dimension of the body L, the temperature rise ΔT, and the coefficient of thermal expansion α. If L = 1m and ΔT = 100 ^oC, $\alpha = 10*10^{-6}$ per ^oC, the change in dimension is 10^{-3}m, which is negligible in problems of heat conduction.

The equivalent temperature changes to the estimated drying shrinkage strains may be calculated using the following simple relation:

$$\Delta T_{DS} = \frac{\varepsilon_{sh}}{\alpha_c} \tag{20}$$

where,

ΔT_{DS} = drying shrinkage equivalent temperature change,

ε_{sh} = shrinkage strain, and

α_c = coefficient of thermal expansion of concrete.

Then the equivalent temperature changes to drying shrinkage may be added algebraically to the temperature changes resulting from thermal analysis. The effect of this sum of temperatures, which appears as thermal stress and strain, may be

Detected using the second method described in (2) above. This means that the problem is treated as "an initial stress or strain" problem. The term *"initial stress"* signifies a stress present before deformations are allowed. Effectively, it is a residual stress to be superposed on stress caused by deformation. The effect of temperature changes can be placed as initial strain ε_o, or initial stress and strain σ_o and ε_o. Both are viewed as alternative ways to express the same thing (Cook, 1989).

In a linear elastic material, the stress-strain relation is (Cook, 1989):

$$\varepsilon = \frac{\sigma}{E} + \varepsilon_o \tag{21}$$

where,

ε_o = initial strain = $\alpha_c \Delta T$

or,

$$\sigma = E(\varepsilon - \varepsilon_o) \tag{22}$$

The strain energy U_o is defined as (Cook, 1989):

$$U_o = \int_v \frac{\sigma\varepsilon}{2} dv \tag{23}$$

Substituting eq. (22) into eq. (23):

$$U_o = \int_v \frac{E}{2} (\varepsilon - \varepsilon_o)^2 dv$$

or,

$$U_o = \int_v \frac{E}{2}\left(\varepsilon^2 - 2\varepsilon\varepsilon_o + \varepsilon_o^2\right)dv \quad (24)$$

The third term in the parenthesis in eq. (24) can be omitted since it is independent of nodal displacements. Then its derivative is equal to zero. Thus,

$$U_o = \int_v \frac{E}{2}\left(\varepsilon^2 - 2\varepsilon\varepsilon_o\right)dv \quad (25)$$

Writing $u_o = \frac{E}{2}\left(\varepsilon^2 - 2\varepsilon\varepsilon_o\right)dv$ = is the energy per unit volume. Hence, for a state of multiaxial stresses:

$$u_o = \frac{1}{2}\lfloor\varepsilon\rfloor[D]\{\varepsilon\} - \lfloor\varepsilon\rfloor[D]\{\varepsilon_o\} \quad (26)$$

where

[D] = the constitutive relations matrix for concrete and is defined for linear-elastic material as follows (Cook, 1989):

$$[D] = \frac{E}{(1+\upsilon)(1-2\upsilon)}\begin{bmatrix} (1-\upsilon) & \upsilon & \upsilon & 0 & 0 & 0 \\ \upsilon & (1-\upsilon) & \upsilon & 0 & 0 & 0 \\ \upsilon & \upsilon & (1-\upsilon) & 0 & 0 & 0 \\ 0 & 0 & 0 & \frac{1-2\upsilon}{2} & 0 & 0 \\ 0 & 0 & 0 & 0 & \frac{1-2\upsilon}{2} & 0 \\ 0 & 0 & 0 & 0 & 0 & \frac{1-2\upsilon}{2} \end{bmatrix} \quad (27)$$

The potential of external load may be expressed as:

$$\Omega_{ex} = -\lfloor u\rfloor\{\phi\} \quad (28)$$

where,

$\lfloor u\rfloor$ = the displacement field vector, and

$\{\phi\}$ = the load vector.

Furthermore, the potential of body forces is given by:

$$\Omega_{bf} = \lfloor u\rfloor\{\overline{F}\} \quad (29)$$

Where, $\{\overline{F}\}$ = the body force vector, which is any force distributed over the entire volume of the body like the self-weight.

The total potential energy per unit volume can be written in the form (Cook, 1989):

$$\begin{aligned}\Pi_{p_0} &= U_o + \Omega \\ &= \frac{1}{2}\lfloor\varepsilon\rfloor[D]\{\varepsilon\} - \lfloor\varepsilon\rfloor[D]\{\varepsilon_o\} - \lfloor u\rfloor\{\phi\} - \lfloor u\rfloor\{\overline{F}\}\end{aligned} \quad (30)$$

The total potential within the element is:

$$\Pi_{p_e} = \int_v \Pi_{p_o}\, dv \quad (31)$$

or,

$$\begin{aligned}\Pi_{p_e} &= \frac{1}{2}\int_v \lfloor\varepsilon\rfloor[D]\{\varepsilon\}dv - \int_v \lfloor\varepsilon\rfloor[D]\{\varepsilon_o\}dv \\ &- \int_s \lfloor u\rfloor\{\phi\}ds - \int_v \lfloor u\rfloor\{\overline{F}\}dv\end{aligned} \quad (32)$$

Since,

$$\{u\} = [N]\{e\} \quad (33)$$

where,

[N] = shape function matrix, and

{e} = nodal displacement vector.

Also,

$$\{\varepsilon\} = [B]\{e\} \quad (34)$$

where,

[B] = strain-nodal displacement matrix.

Hence,

$$\Pi_{p_e} = \frac{1}{2}\int_v \lfloor e \rfloor [B]^T [D]\{e\}dv - \int_v \lfloor e \rfloor [B][D]\{\varepsilon_o\}dv - \int_s \lfloor e \rfloor [N]^T \{\phi\}ds - \int_v \lfloor e \rfloor [N]\{\bar{F}\}dv \quad (35)$$

which after simplification and introducing effects of externally applied nodal forces becomes:

$$\Pi_{p_e} = \frac{1}{2}\lfloor e \rfloor [K]\{e\} - \lfloor e \rfloor \{R\} - \lfloor e \rfloor \{F\} \quad (36)$$

where, {F} = externally applied nodal forces vector.

Applying the minimization of the total potential yields:

$$\frac{\partial \Pi_p}{\partial \{e\}} = 0$$

or,

$$[K]\{e\} = \{F\} + \{R\} \quad (37)$$

where,

$$\{R\} = \int_v [B]^T [D]\{\varepsilon_o\}dv + \int_v [N]^T \{\bar{F}\}dv + \int_s [N]^T \{\phi\}ds$$

Eq. (37) will be used in the analysis of the mass concrete due to effects of temperature and drying shrinkage volume changes.

Computer Implementation

Besides the "Graphical User Interface (GUI)" that is commonly used in software packages, ANSYS program proposes a programming language similar to some extent to the conventional FORTRAN language. The proposed language is referred as APDL (ANSYS Parametric Design Language).

A modified ANSYS program is adopted in this study. This consists of a main program and four subprograms. The main program contains the principal steps of analysis and required calls for subprograms. Each of these subprograms is responsible of some limit tasks like:

- Performing the thermal analysis,
- Storing temperature values in a pre-dimensioned array,
- Calculating drying shrinkage strains throughout the concrete body, and
- Conducting the nonlinear structural analysis by considering the effect of concrete aging via updating concrete strength parameters (f_t', f_c', E_c) after deleting the thermal finite element mesh and constructing a new structural one.

Two Types of elements are used in this program:

1. Thermal Solid 70: This element is an eight-noded brick element with one degree of freedom, temperature, at each node. The element is applicable to a three-dimensional, steady state or transient thermal analysis.

2. Structural Solid 65: This element is used for the three-dimensional modeling of the concrete with or without reinforcing bars. The element is defined by eight nodes having three degrees of freedom at each node: translations in the global x, y, and z directions. It is capable of considering cracking in tension and crushing in compression.

Problem Description and Results

To investigate the effect of the transverse base restraint on the cracking behavior of mass concrete member having the dimensions shown in Fi.(3) due to temperature variation and drying shrinkage volume changes, a nonlinear finite element analysis was applied to base restrained thick plain concrete slab resting on the soil. Four different aspect ratios (width/length) were considered for the case of a slab with fixed bottom cast at the first of January (winter concrete placement) in Baghdad. The aspect ratios were 0.2, 0.4, 0.8, and 1.0 and obtained by fixing the length of the slab to 10 meters and varying the width as 2, 4, 8, and 10 meters. In all these cases, the thickness of the slab was taken as 1.5 m. The properties of the concrete tht adopted during analysis were listed in Table(2).

Thermal and structural analyses were conducted on the slab including all the surrounding circumstances and boundaries utilizing the finite element mesh shown in Fig. (3).

The temperature distribution in the central sections along the length and width directions at some times after concrete placement are shown in Figs. (4) to (15). The assessed final cracking pattern of the concrete slabs with different aspect ratios can be seen in Figs. (16) to (19).

Conclusions

The following conclusions can be drawn from the results of analysis:

1. Value of peak temperature increases with increasing aspect ratio (B/L) of the slab especialy at age of 3days after concrete placement as shown in Figs. (4), (7), (10) and (13). This may be related to the increase in the magnitude of heat generated upon concrete placement due to volume increase.
2. A small temperature drop at the 28^{th} day of concrete age is noticed as the ratio B/L is increased (see Figs.((5), (8), (11) and (14). This is attributed by the effect of the volume to surface ratio (V/S), since the temperature increases with increasing the aspect ratio (B/L).
3. The number of primary cracks (cracks that extend over the entire thickness) increase with increasing the width of slab, i.e., the aspect ratio as shown in Figs(16), (17) and (18). This can be interpreted as a result of the considerable increase in restraint provided by the slab base and the increase in the maximum temperature due to the hydration process after concrete placement.
4. The full-depth cracks are concentrated at the central portion of the slab where the maximum drop in temperature occurs (Figs.(16) to (19).

From the above and since it was concluded previously that the major cause of cracking in the thick slabs is temperature drop, the effect of the third dimension (width) cannot be ignored when the response (stresses and cracking) of this type of structures is required. Unfortunately, most of the standards like ACI-Committee neglect the effect of the third dimension and assume a uniform temperature distribution.

REFRENCES

ACI Committee 207, "Effect of Restraint, Volume Change, and Reinforcement on Cracking in Massive Concrete", (ACI 207.2R-95). American Concrete Institute, Detroit, 1999, 26 pp

.ACI Committee 209, "Prediction of Creep, Shrinkage, and Temperature Effects in Concrete Structures", (ACI 209R-92), (Reapproved 1997). American Concrete Institute, Detroit, 1999, 47 pp.

ANSYS 5.4 Inc., "ANSYS Theory Reference", Eighth Edition, SAS IP, Inc. 1997, Chapter 4 pp. 48-56.

Carlson, R. W., "Drying Shrinkage of Large Concrete Members" ACI Journal, Proceedings, Vol. 33, January-February 1937, pp.327-336.

Cook, R. D., Malkas, D. S., and Plesha, M. E., "Concepts and Applications of Finite Element Analysis", John Wiley and Sons Inc., Third edition, 1989, 630 pp.

Fung, Y. C., "Foundations of Solid Mechanics", Prentice-Hall Inc., Englewood Cliffs, New Jersey, 1965, 525 pp.

Holman, J. P., "Heat Transfer", Fourth Edition, 1976, McGraw-Hill.

Kammouna, Z. M., "Development of A Mathematical Model for Creep of Concrete with Reference to Baghdad Climate", M.Sc. Thesis, Baghdad University, College of Engineering, 2001, 90 pp.

Willam, K. J., and Warnke, E. D., "Constitutive Model for the Triaxial Behavior of Concrete", Proceedings, International Association for Bridge and Structural Engineering, Vol. 19, ISMES, Bergamo, Italy, p. 174 (1975).

Table (1) Drying shrinkage strains

d/H (*)	Drying shrinkage strain (10^{-6})																			
	Slab width = 2.0m					Slab width = 4.0m					Slab width = 8.0m					Slab width = 10.0m				
	After … days					After … days					After … days					After … days				
	8	14	28	90	180	8	14	28	90	180	8	14	28	90	180	8	14	28	90	180
0	0.5	3.2	7.5	18.0	24.3	0.2	1.3	3.0	7.1	9.6	0. 1	0.6	1.4	3.3	4.4	0.08	0.48	1.12	2.7	3.6
0.2	0.2	1.3	3.1	7.5	10.3	0.1	0.5	1.2	3.0	4.1	0.04	0.25	0.57	1.4	1.9	0.03	0.2	0.47	1.13	1.5
0.4	0.07	0.4	1.01	2.4	3.2	0.03	0.17	0.4	0.96	1.3	0.01	0.08	0.19	0.44	0.63	0.01	0.07	0.15	0.36	0.48
0.6	0.02	0.1	0.3	0.8	1.1	0.01	0.05	0.12	0.3	0.45	0	0.02	0.05	0.14	0.21	0	0.02	0.04	0.11	0.17
0.8	0	0	0	0	0	0	0	0	0	0	0	0	0	0	0	0	0	0	0	0
1.0	0	0	0	0	0	0	0	0	0	0	0	0	0	0	0	0	0	0	0	0

(*) d/H defines the ratio of the depth from top surface / the slab thickness H.

Table (2) Material Properties

Property		Unit	Values for	
			Concrete	Soil
Thermal	Conductivity, k	kJ/m.day.^{o}C	240	72
	Speecific heat, c_p	kJ/kg.^{o}C	1.0	0.92
Physical & Mechanical	Density, ρ	Kg/m^3	2400	1700
	Modulus of elasticity, E	MPa	23168(*)	1000
	Poisson's ratio, ν	-	0.15	0.40
	Compressive strength, f_c'	MPa	21(*)	-
	Tensile strength, f_t'	MPa	1.55(*)	-
	Coefficient of thermal expansion, α	/^{o}C	12×10^{-6}	0.3×10^{-6}
	Cohesion, c	MPa	4.7(*)	0.1
	Angle of internal friction, ϕ	degrees	41.7(*)	20

(*) The values were assumed or caculated at the age of 28days

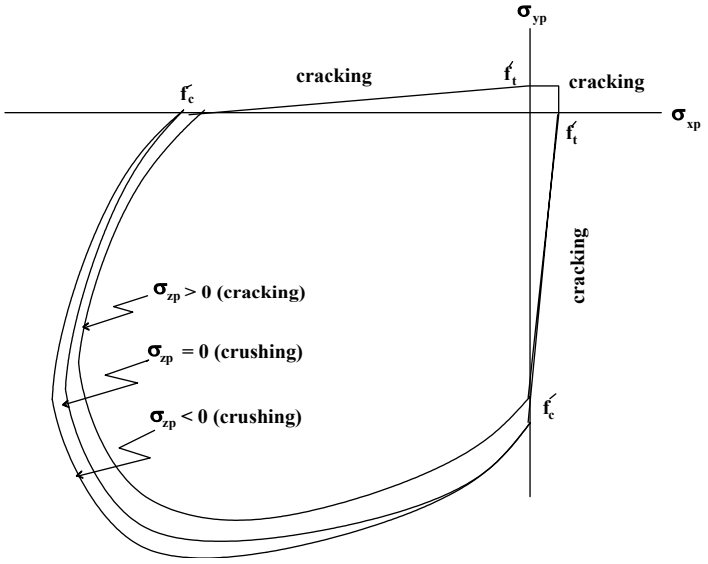

Fig.(1): Failure surface in principal stress space with nearly biaxial stress state, after ANSYS Inc.

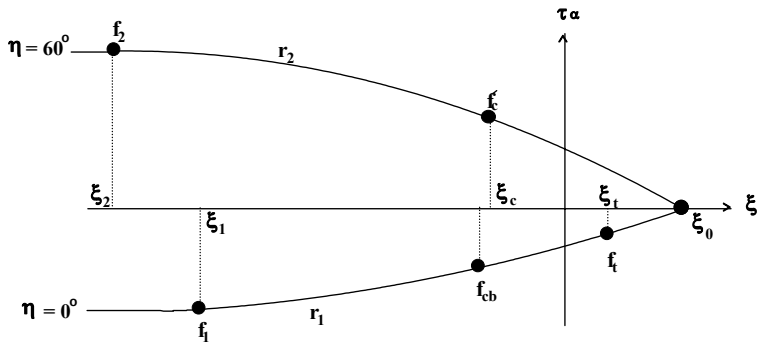

Fig. (2): A profile of the failure surface, after ANSYS Inc.

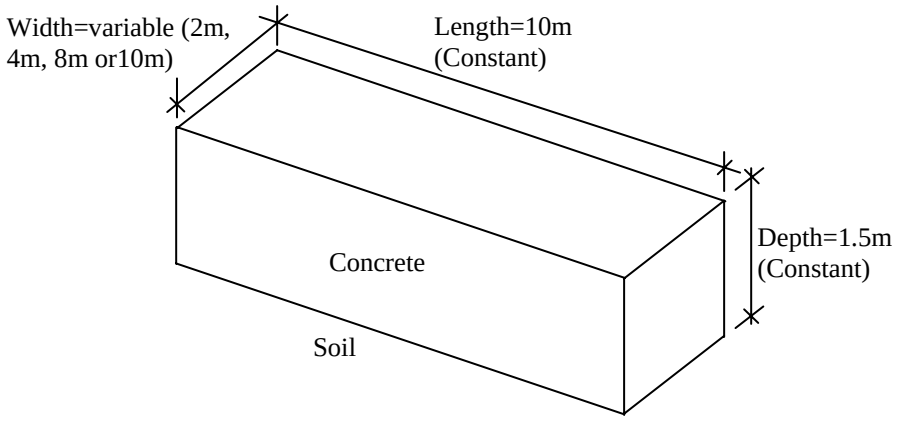

Fig. (3): Problem Geometry.

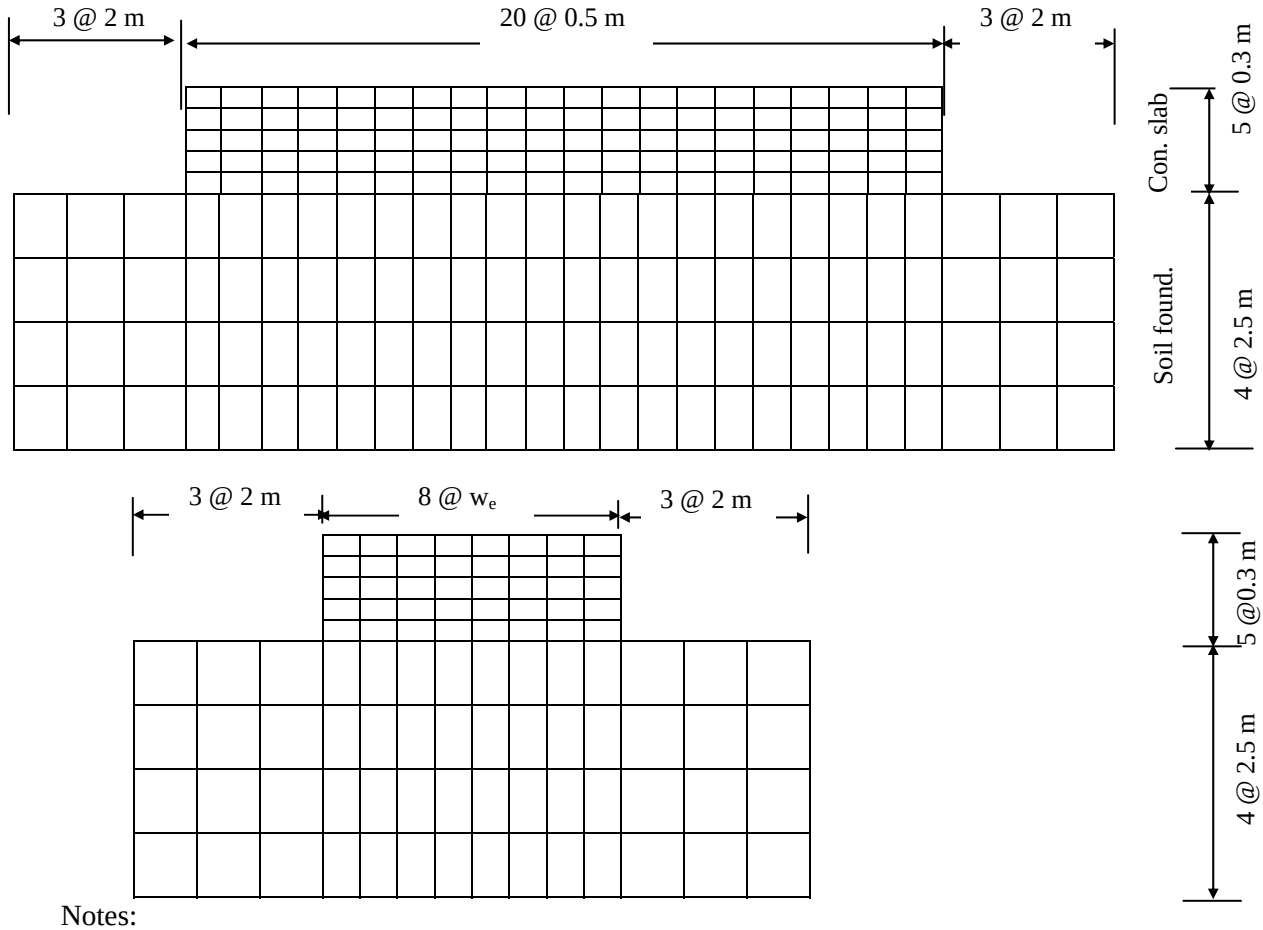

Notes:

- w_e = concrete element width (variable) = 0.25, 0.5, 1.0, or 1.5 m.
- Dimensions are not to scale.

Fig. (3): Finite element mesh for a thick concrete slab problem

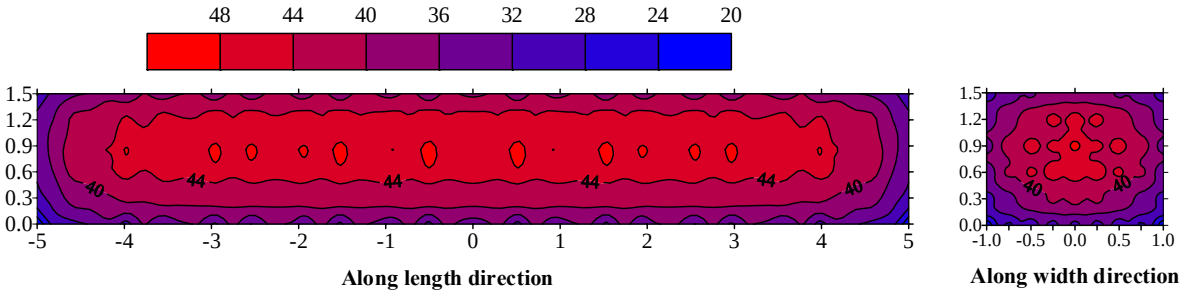

Note: Temperatures are in ^{o}C

Fig. (4): Temperature distribution in a slab with B/L=0.2 (3 days after placement)

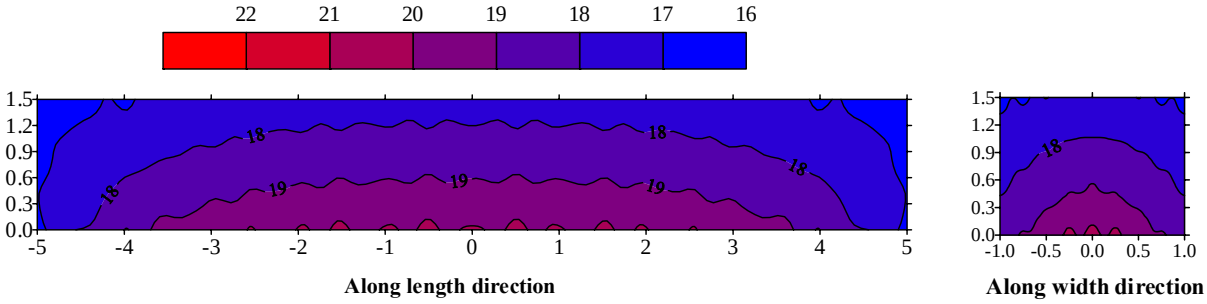

Note: Temperatures are in ^{o}C

Fig. (5): Temperature distribution in a slab with B/L=0.2 (28 days after placement)

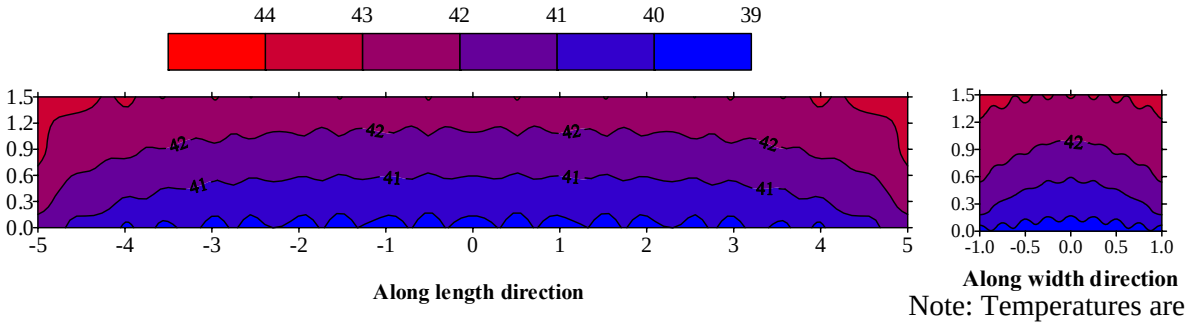

Note: Temperatures are in ^{o}C

Fig. (6): Temperature distribution in a slab with B/L=0.2 (180 days after placement)

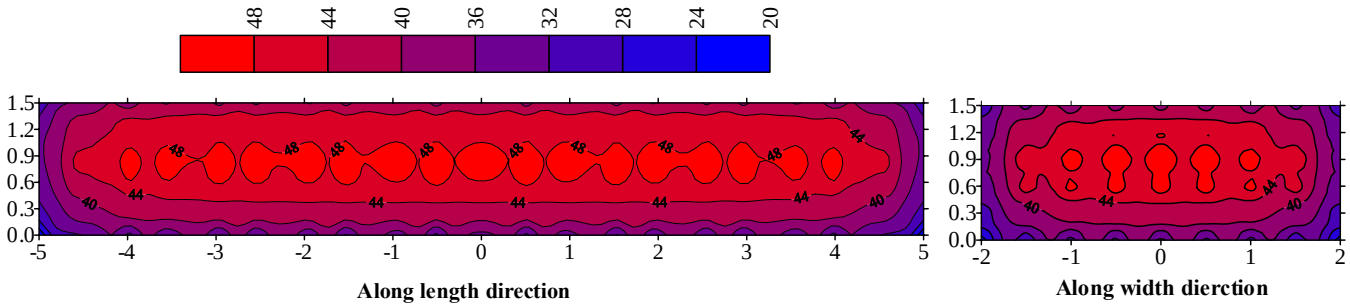

Note: Temperatures are in ^{o}C

Fig. (7): Temperature distribution in a slab with B/L=0.4 (3 days after placement)

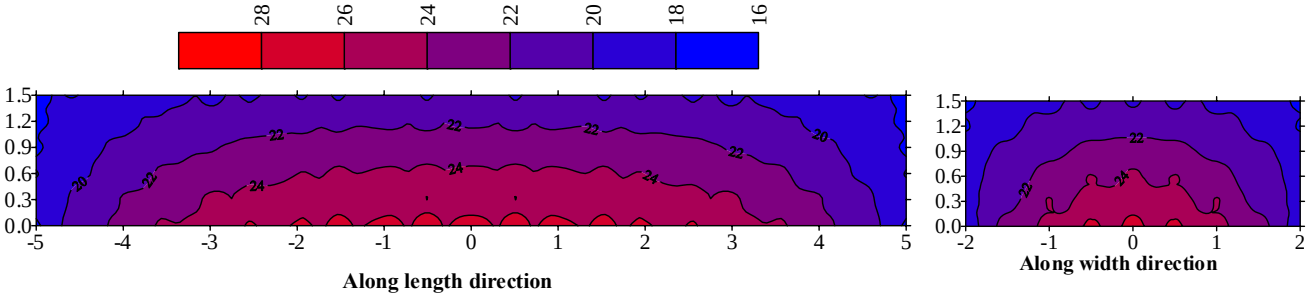

Note: Temperatures are in ^{o}C

Fig. (8): Temperature distribution in a slab with B/L=0.4 (28 days after placement)

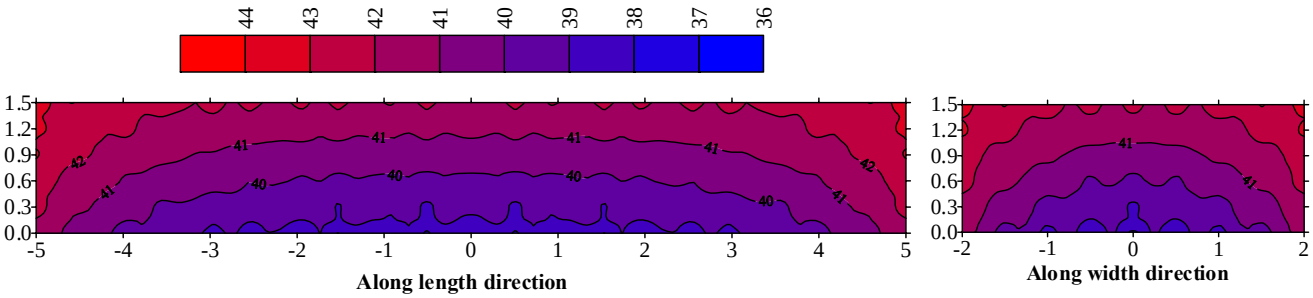

Note: Temperatures are in ^{o}C

Fig. (9): Temperature distribution in a slab with B/L=0.4 (180 days after placement)

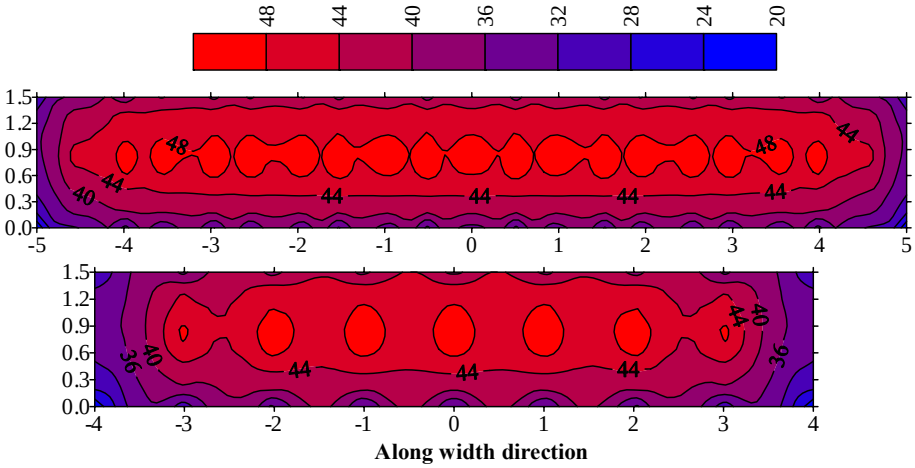

Note: Temperatures are in ^{o}C

Fig. (10): Temperature distribution in a slab with B/L=0.8 (3 days after placement)

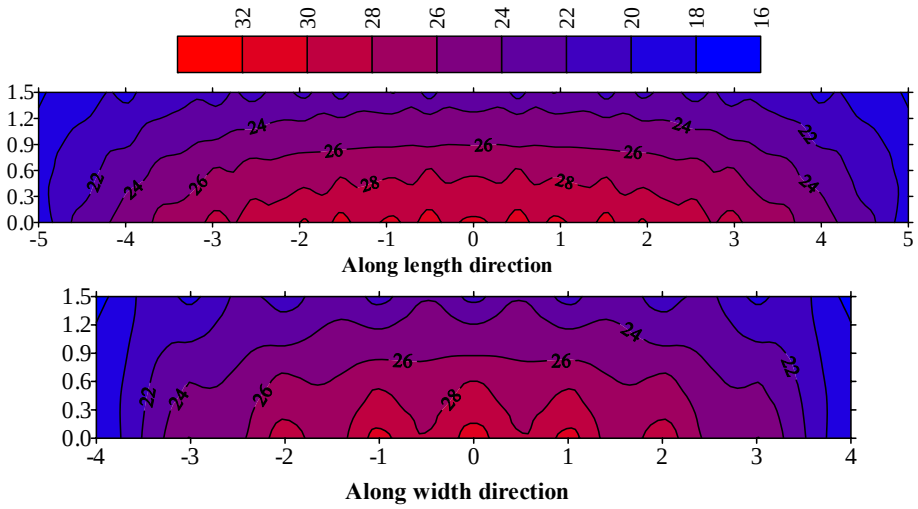

Note: Temperatures are in ^{o}C

Fig. (11): Temperature distribution in a slab with B/L=0.8 (28 days after placement)

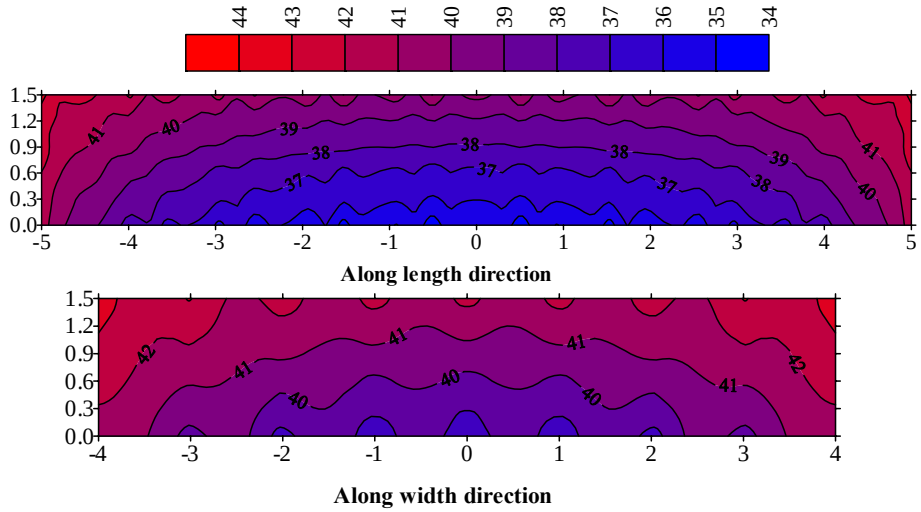

Note: Temperatures are in ^{o}C

Fig. (12): Temperature distribution in a slab with B/L=0.8 (180 days after placement)

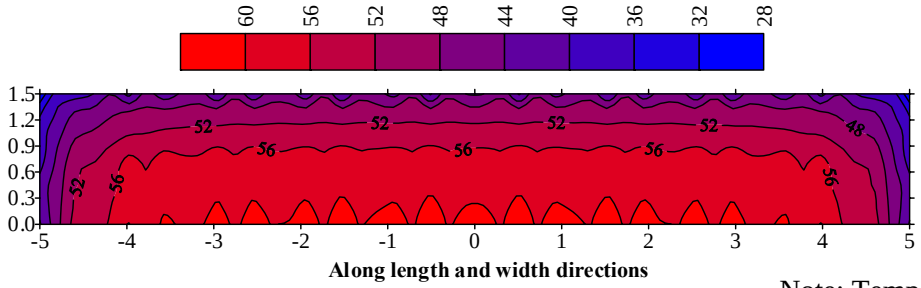

Note: Temperatures are in ^{o}C

Fig. (13): Temperature distribution in a slab with B/L=1.0 (3 days after placement)

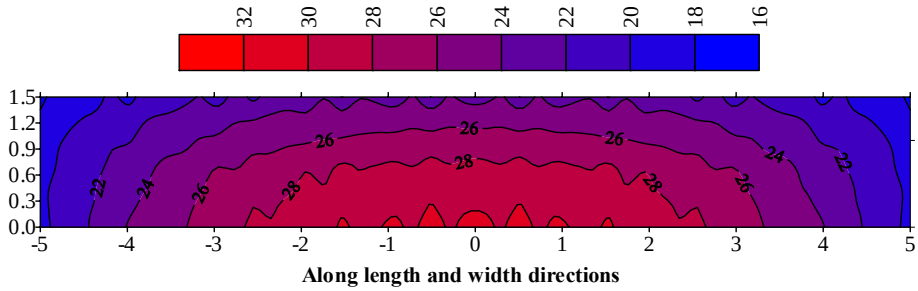

Note: Temperatures are in ^{o}C

Fig. (14): Temperature distribution in a slab with B/L=1.0 (28 days after placement)

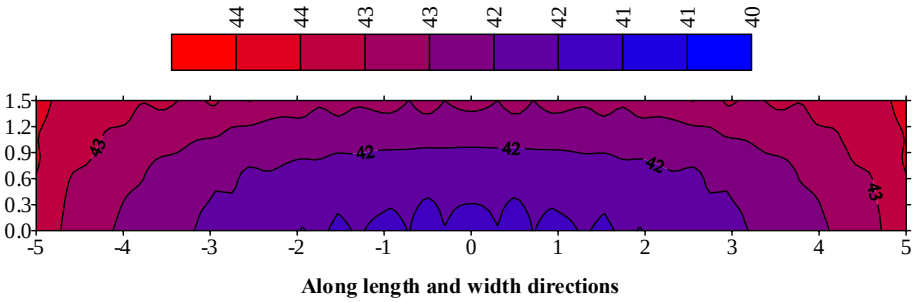

Note: Temperatures are in ^{o}C

Fig. (15): Temperature distribution in a slab with B/L=1.0 (180 days after placement)

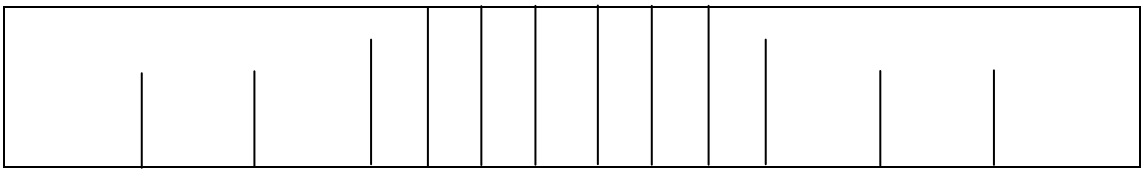

Side view of the central section along length direction

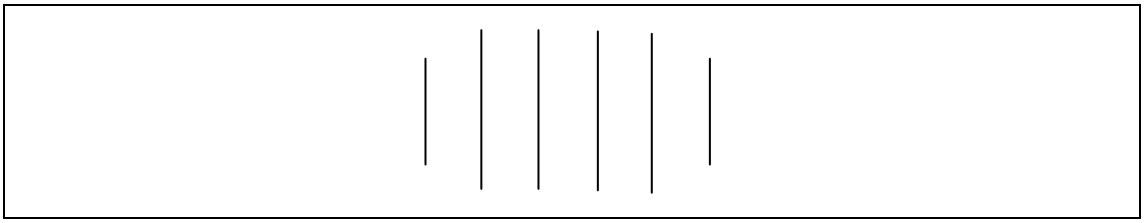

Top view

Fig. (16): Final cracking pattern for slab cast in winter with B/L=0.2

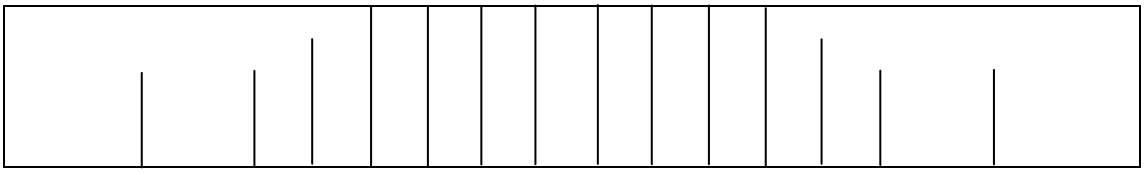

Side view of the central section along length direction

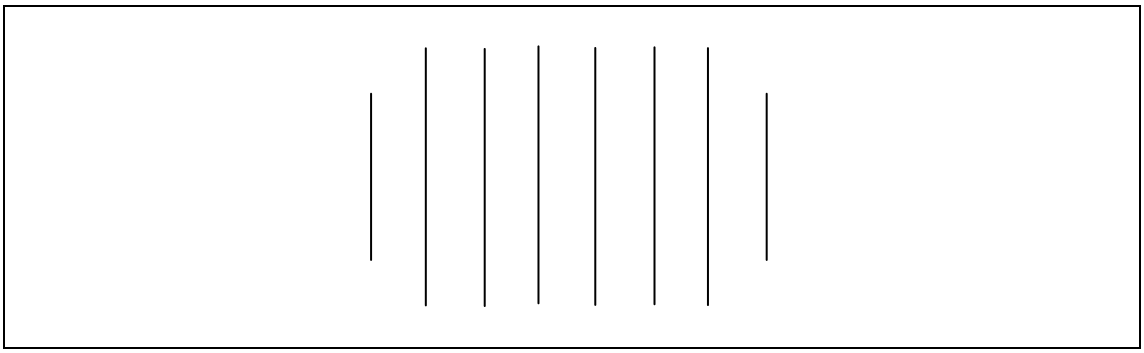

Top view

Fig. (17): Final cracking pattern for slab cast in winter with B/L=0.4

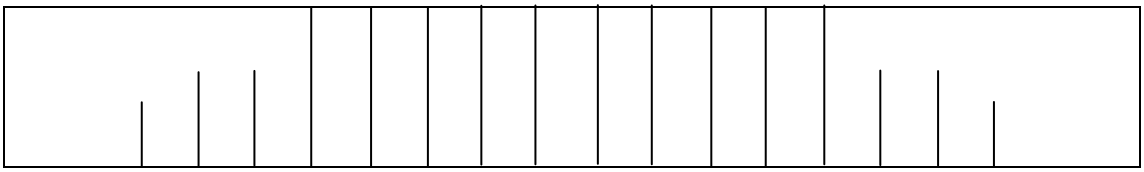

Side view of the central section along length direction

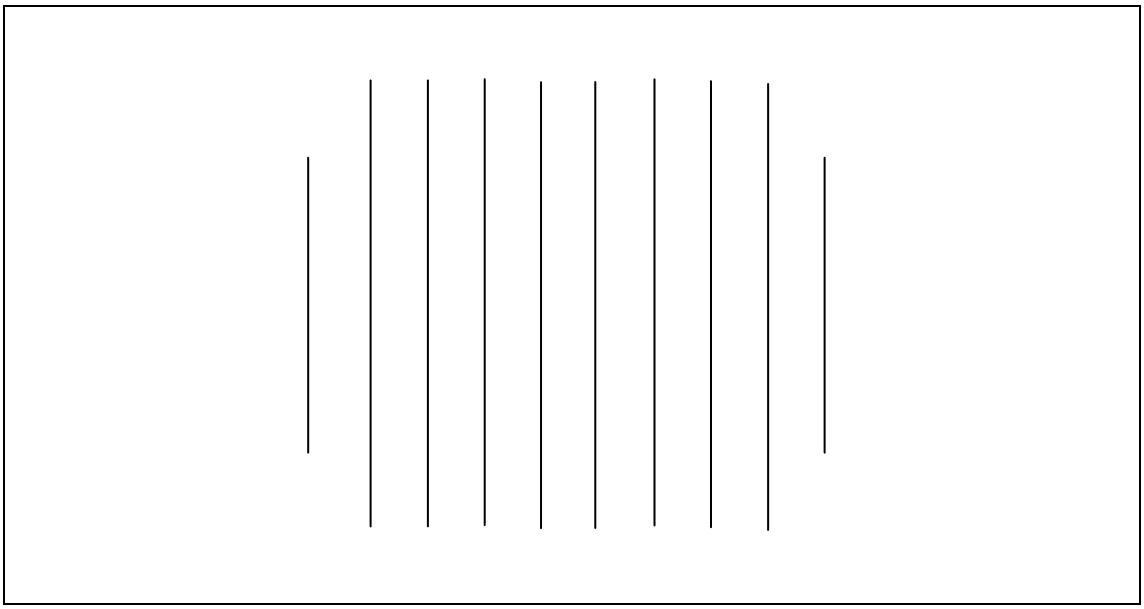

Top view

Fig. (18): Final cracking pattern for slab cast in winter with B/L=0.8

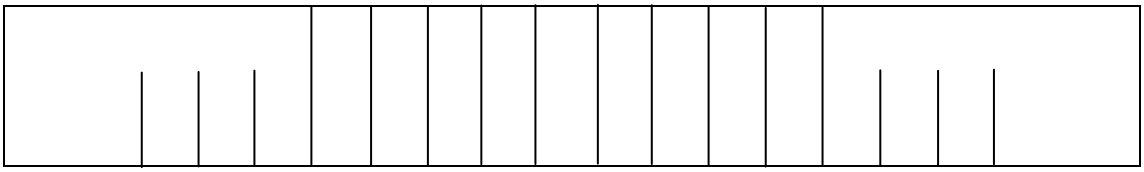

Side view of the central section along length direction

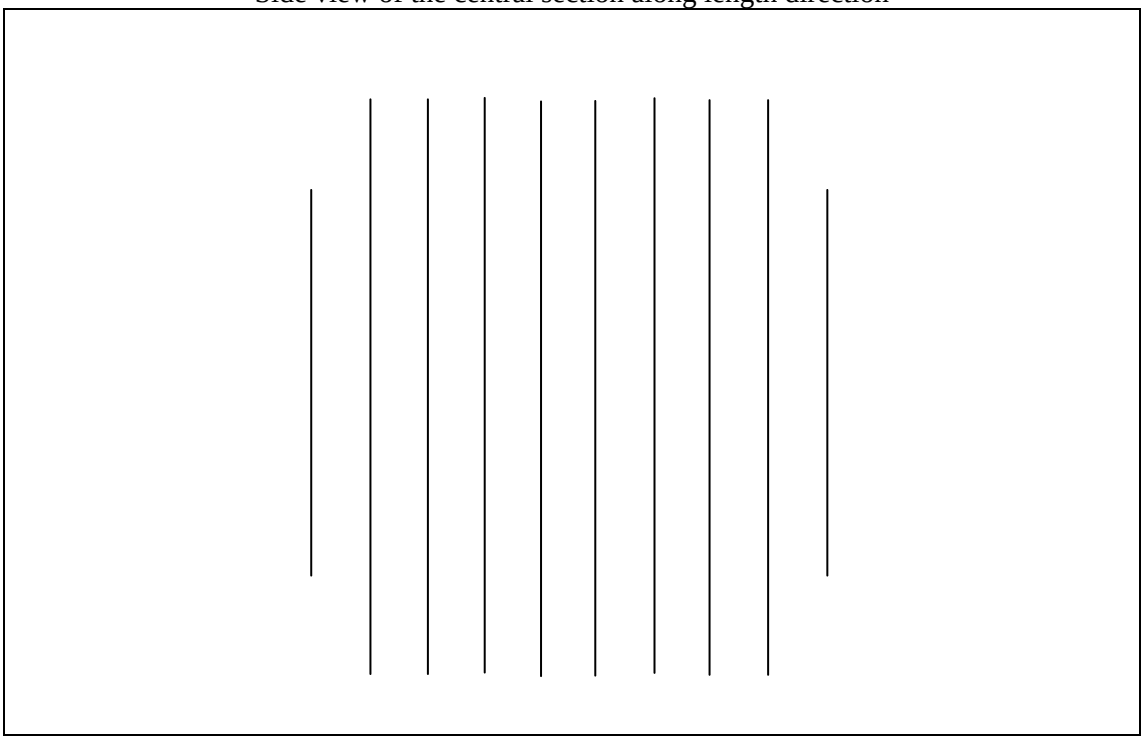

Top view

Fig. (19): Final cracking pattern for slab cast in winter with B/L=1.0